International Journal of Aquatic Science
ISSN: 2008-8019
Vol 12, Issue 02, 2021

Mapping LULC changes of the coastal Kanyakumari district, Tamil Nadu, India Using Geospatial technology

ARAN CASTRO A J[1], KUMAR R S[2], JUSTINE K ANTONY[3], Karan Ram[4], PAGARE N S[5], PRAVEEN RAJ R[6], P.RAJ KUMAR[7]

[1]PhD. Research Scholar, Department of Earth Sciences, Annamalai University, Tamil Nadu, India
[2]Professor, Department of Earth Sciences, Annamalai University, Tamil Nadu, India
[3]PhD. Research Scholar, Department of Earth Sciences, Annamalai University, Tamil Nadu, India
[4]M.Sc. Geology, Department of Earth Sciences, Annamalai University, Tamil Nadu, India
[5]PhD. Research Scholar, Department of Earth Sciences, Annamalai University, Tamil Nadu, India
[6]PhD. Research Scholar, Department of Earth Sciences, Annamalai University, Tamil Nadu, India
[7]Project Associate, Centre for Earth Sciences, Indian Institute of Science, Bangalore, Karnataka, India

Email: [1]arancastro17@gmail.com, [2]rskgeoo@gmail.com, [3]justinekantony@gmail.com, [4]karanramiz50@gmail.com, [5]narendra19gis@gmail.com, [6]geopraveenraj@gmail.com, [7]prajkumar@iisc.ac.in

Abstract: Kanyakumari is the southernmost coastal district of India and the state of Tamil Nadu. Due to the rapid increase in the population, the district's land use and land cover areas experience enormous changes in the past few years. So, the study of Land Use and Land Cover Changes in the district is much required for the current scenario. Landsat 8 images were used for the supervised classification.

The cultivable cropland, barren land, beachface landcover and dune cover vegetation decrease in their area because of the rapid growth of urbanisation. The Fallow land, the plantation, saltpans, built-up area and the beach mining areas show an increasing trend in their areas in the study area. The plantation, the fallow land and the beach mining only increase a little in their area, but the saltpans and the built-up areas increase rapidly. The rapid increase of the saltpans and the built-up area show rapid urbanization in the study area. The unfettered changes in the LULC feature are alarming the coastal vulnerability in the Kanyakumari districts coastal villages. This study offers pilot information for sustainable coastal management and suggests planning to decrease coastal regions' risk and vulnerability.

Keywords: Land use, Land cover, LandSat, Urbanisation, Coastal and Classification

1. INTRODUCTION:

From the existence of civilisation, human settlements were established along the coastal regions of various continents. It provided multiple opportunities for trading and an easy way of transportation by sea and oceans. Thus, the coastal zones were found to be densely populated., 47.2% of the world population live in urban settlements and generate pollution to the nearby coastal areas from natural processes such as reclamation, dredging and waves, tides, and the anthropogenic process like municipal sewage, urban and industrial activities. Public pressure on coastal zones worldwide has increased dramatically in the last 50 years (Santhiya, 2010). Besides global economic integration, coastal superiority in rich resources and convenient traffic is more diverse, quickening the coastal region’s urbanisation course (Xu et al., 2009). Because of the rapid advancement of urbanisation, the coastal areas have undoubtedly experienced land-use and land cover changes (Kurt, 2013). Land use and land cover changes are possibly the reason for the major global environmental change since they occur at spatial and temporal scales directly relevant to our daily existence (Roy & Roy, 2010). In recent times, the Kanyakumari district in southern India experienced notable changes in land-use and landcover features due to marine and terrestrial factors and human activities (Chandrasekar, 2013; Kaliraj et al., 2017a). Kanyakumari is the southernmost coastal district of peninsular India in the state of Tamil Nadu. It has one of the most thickly populated coasts among the districts in the states of India. The coast occupies a heavy concentration of fisher-society, nearly one village for every 1.5 km (Natesan & Parthasarathy, 2010). This fisher-society has constructed many built-ups all along the coast. Because of the increase in population and the built-up areas, the district’s land cover has also experienced enormous changes in the past years. Among these changes, land use/land cover change is widely recognised as an essential aspect of global environmental change, which plays a pivotal role in regional socio-economic development (Xiuwan, 2002). So, the study of LULC changes in the Kanyakumari district is much required for the current scenario.

Therefore, satellite remote-sensing techniques have been broadly used in identifying and supervising land cover change at various scales with valid results (Gilmore et al., 2008). Remote sensing techniques combined with Geographic Information System are crucial in assessing land use and land cover changes (Attri et al., 2015). Remote sensing Satellites with Multi-temporal and high spatial resolution support the LULC study because of their quick revisit time to a particular location and high-resolution images. Landsat series of remote sensing satellites is one of the satellites with the multitemporal resolution and the 30m spatial resolution. Significant works of literature have reported Land use and Land cover changes studies using Landsat Imagery series of satellites (Avery & Berlin, 1992; Wickware & Howarth, 1981; Alam et al., 2002; Chandrasekar et al., 2000; Jaiswal et al., 1999; Jayappa et al., 2006; Kaliraj et al., 2017; Mujabar & Chandrasekar, 2012; Santhiya, 2010; Sharma et al., 2018; Sekertekin et al., 2017; Deng et al., 2019; Hua et al., 2017; Nguyen et al., 2018).

Kaliraj et al. (2017) reported LULC changes in the parts of the Kanyakumari district during the periods from 2000 to 2011. Nevertheless, no studies have been carried out to assess the changes that occurred in the entire coastal areas of the Kanyakumari district. Hence, the current study brings out the necessary information for understanding the land-use and land cover changes and transformation in the coastal areas of Kanyakumari district during the periods between 2013 to 2021.

2. Study Area:

The study area covers the entire coast of the Kanyakumari District (Figure 1), Tamil Nadu, India.

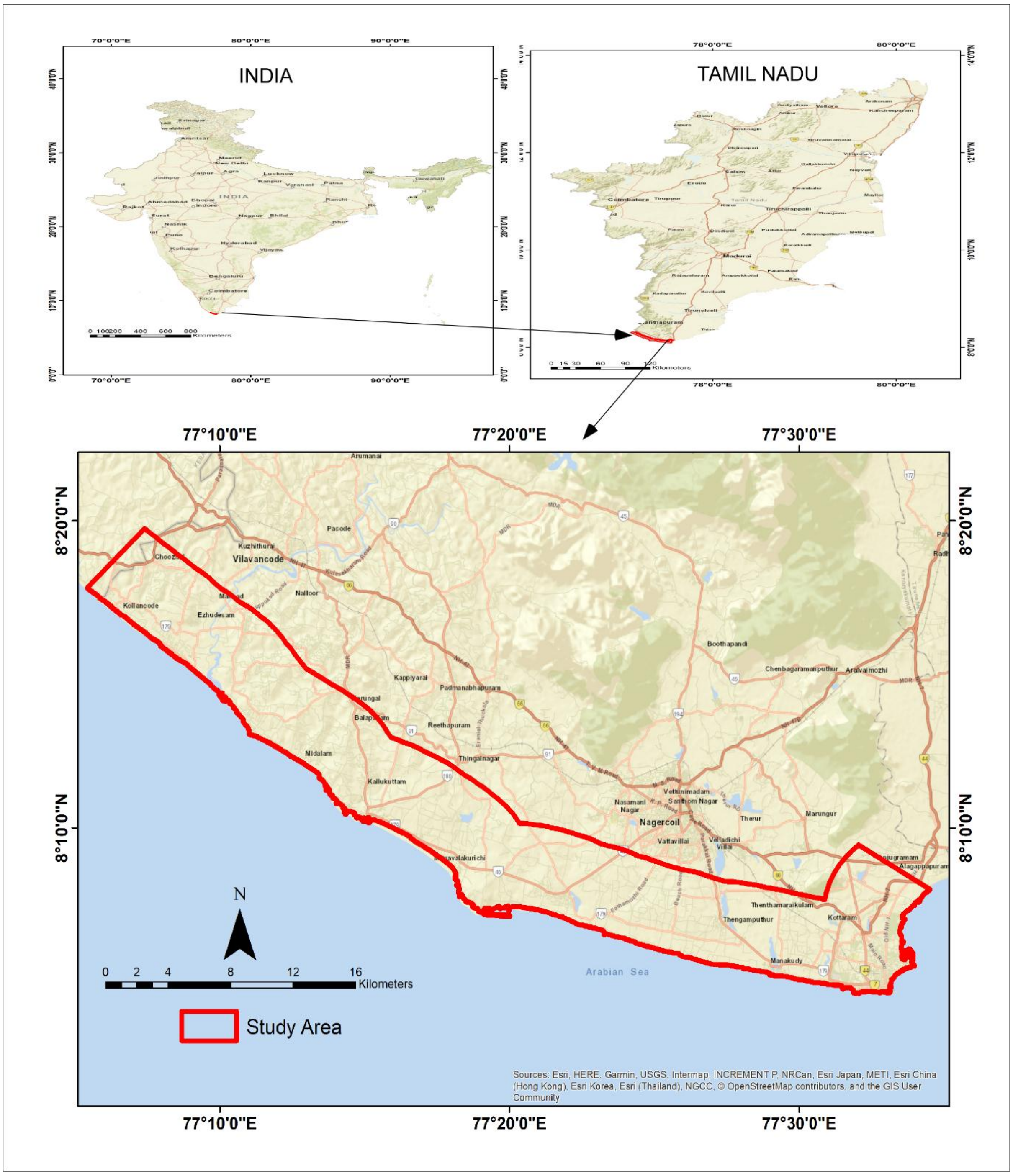

Figure 1 Location map of the study area

2.1 Geography of the study area:

The study area falls in the sub-tropical climate region, with annual rainfall over the district varies from 826 to 1456 mm. The south-eastern part of the district receives low rainfall than the north-western part (Stanley Raj et al., 2017) because of the Western Ghats. The Study area flourishes drainage systems including rivers, streams and water bodies; significant rivers in the study area are Thamiraparani, Valliyar, and Pazhayar. These rivers form various coastal and alluvial landforms at the mouth of the river. Thamiraparani blends with the sea in the Thengapattanam harbour area; Valliyar drains between the Chinnamuttom and Kadiyapattanam village. Similarly, Pazhayar forms an estuarine environment in the Manakudi village.

2.2 Geology of the study area:
occupy the coastal area in the southwest and south of the Kanyakumari district is occupied by the Tertiary and Quaternary sediments. Limestone is exposed as thin capping in the southwest of Kuzhitura near the coast, bordering Kerala. Quaternary sediments of fluvial, fluviomarine, aeolian and marine origin occupy a width of 3 to 5 km. In the coastal areas, two types of the aeolian process occurred, the red sands and white sands, which form the teris and the coastal dunes.
The topography of the study area is mild, with an elevation not exceeding 60 m at places in the coastal belt where crystalline rocks are highly weathered to laterite. Lateral deposits or bay deposits of sand, zircon, rutile, ilmenite and garnet minerals are widespread phenomena along the entire coast of Kanyakumari, whereas monazite is deposited in the Manavazhakurichi area (Chandrasekharan, 2001). Some of the beaches are rocky, majorly composed of crystalline outcrops made up of khondalite, charnockite, and garnetiferous biotite gneiss.

2.3 Geomorphology of the study area:
Geomorphological forms like sandy beaches (Figure 2a), rocky shores (Figure 2b), dune complexes, estuaries (Figure 2c), wetlands, and shallow marshes (Figure 2d) are found all along the coast of the Kanyakumari district. (Kaliraj et al., 2015). Colachel coastal area comprises a sandy beach and a wide sandy beach found all along the Lemor beach. Rocky shores are mainly found in the Muttom and the Kadiyapattanam area (Figure 2b). In the Rocky shores, the Rocky cliffs (Figure 2f) are present and also, the dominant wave action developed some wave cut notches in the Muttom area. Dune complexes can be seen all along with the coastal regions from Manakudi to the Pallam area. Simultaneously, the estuarine environment is present in the Manakudi area, where the Pazhayar river blends with the Arabian sea (Figure 2c). The other wetlands like Shallow marshes (Figure 2d) and salt pans (Figure 7c) are also present in the Manakudi area. On the western side of the district's coastal villages, the inhabitants build the Sea walls and groins because of the high erosion rate in those areas. Skerry structure is also presents in some parts of the study area (Figure 2e). Especially in Kanyakumari, Swami Vivekananda rock is a well-known skerry structure.

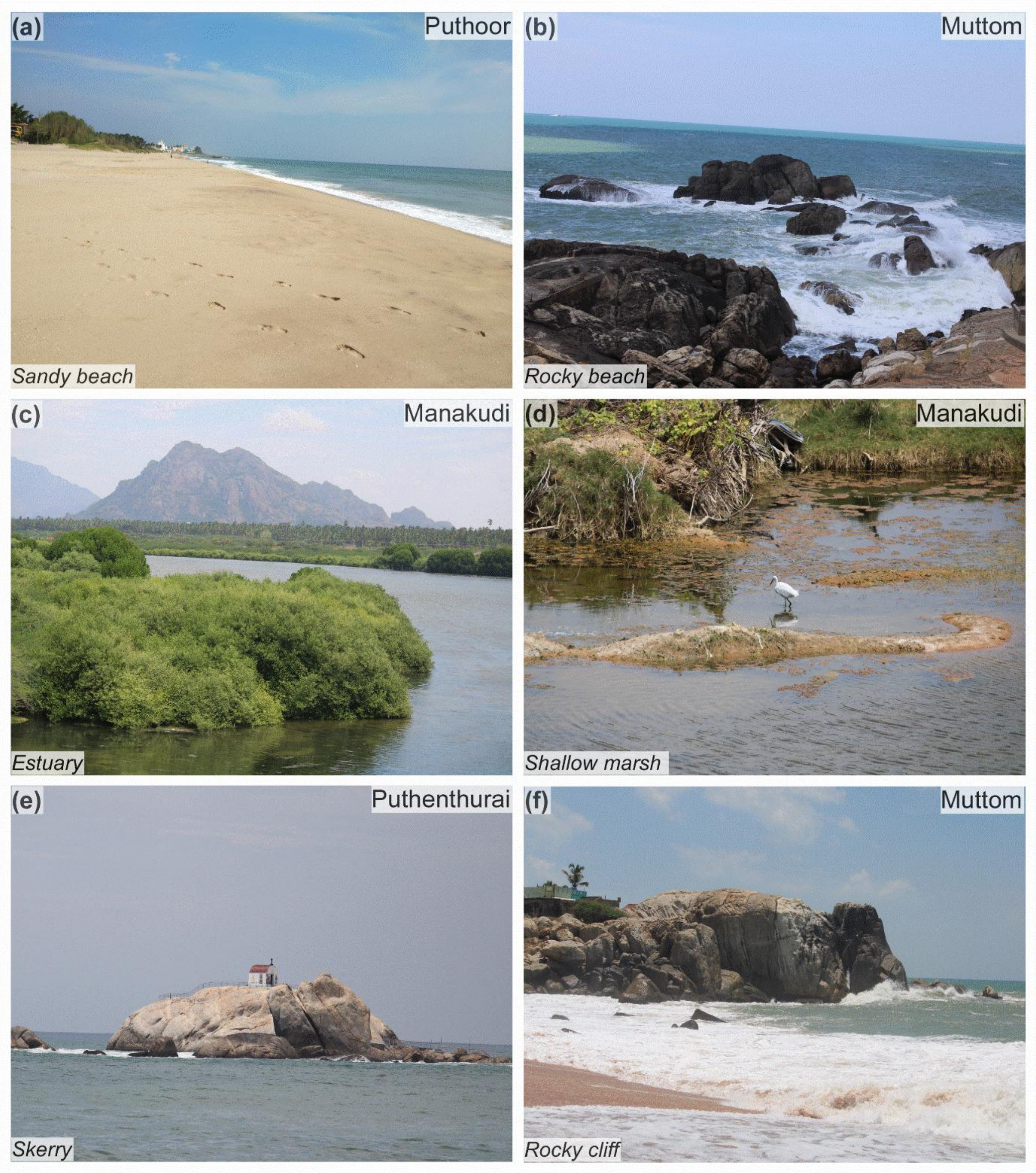

Figure 2 Geomorphological features of the study area

2. MATERIALS AND METHODS

Landsat 8 OLI (Operational Land Imager) data were selected for this study (Table 1).

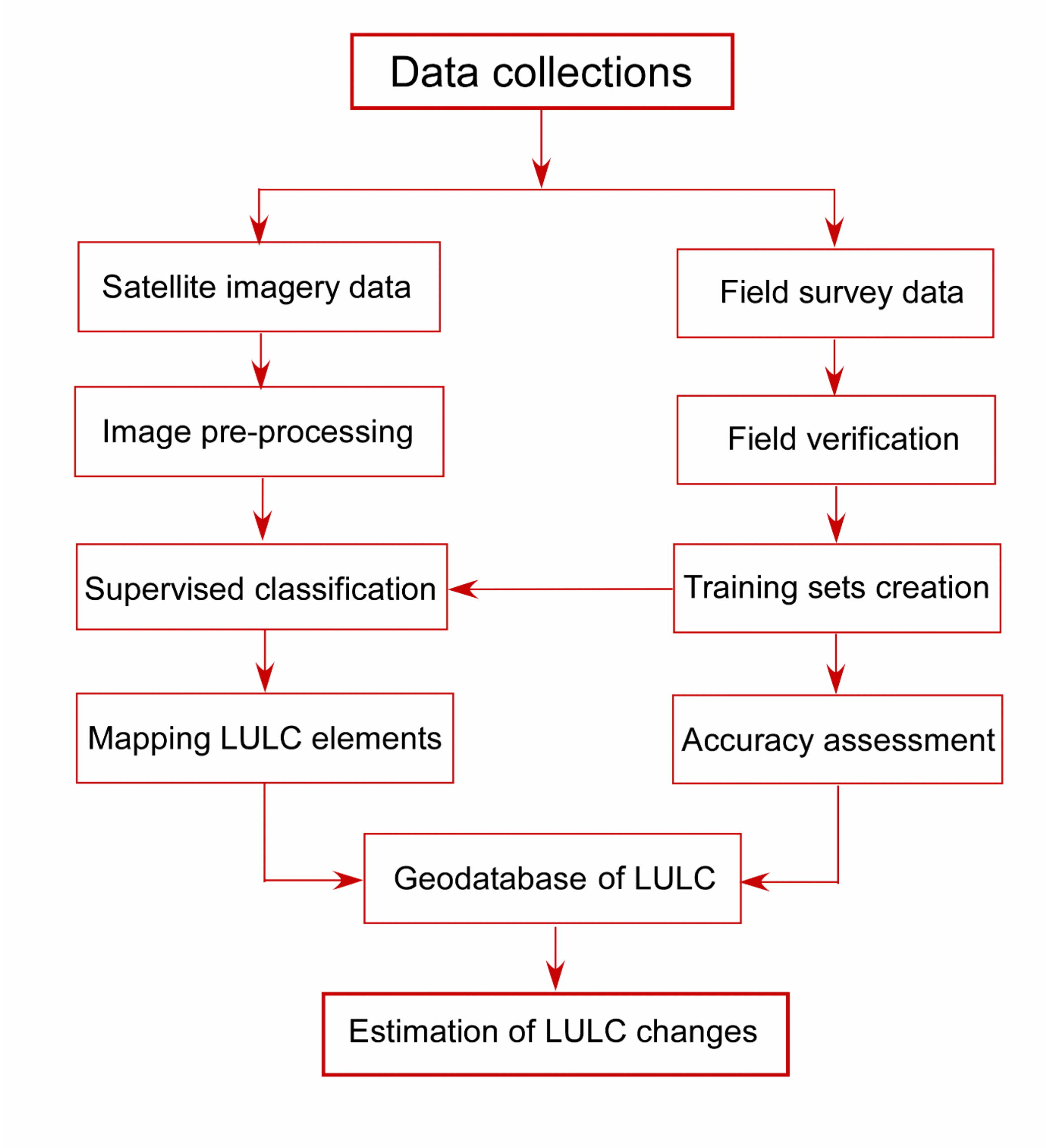

Figure 3 Methodology flow chart

Year	Satellite	Date of Pass	Spectral Resolution	Spatial Resolution
2013	Landsat 8 OLI		11 bands	30m (pan 15m)
2017	Landsat 8 OLI		11 bands	30m (pan15m)
2021	Landsat 8 OLI		11 bands	30m (pan 15m)

Table 1 Details of the selected satellite data

Landsat 8 images were used for the study, with the spectral resolution of coastal aerosol, the visible region, NIR, SWIR, panchromatic & TIRS. The spatial resolution is 30m for band 6 & 9, 60m for band 7, 15m for band 8 and 100m for band 10 & 11 (Table 2).

BANDS	SPECTRAL RESOLUTION	SPATIAL RESOLUTION
1	Coastal aerosol	30m
2	Blue	30m
3	Green	30m
4	Red	30m
5	Near-Infrared (NIR)	30m
6	Short-wave Infrared (SWIR) 1	30m
7	Short-wave Infrared (SWIR) 2	60m
8	Panchromatic	15m
9	Cirrus	30m
10	TIRS 1	100m
11	TIRS 2	100m

Table 2 Details of the LandSat 8 OLI Imagery

The temporal resolution is 16 days for the Landsat 8 OLI satellite. For 2013, 2017 and 2021, the data has been taken for the LULC study. Initially, noise reduction was performed in the satellite data; the median filter method was operated for this purpose. Then the satellite images were geometrically rectified; the pictures were georeferenced with UTM 43N projection. And the data were resampled with the nearest neighbour method. The 15m resolution images were generated by combining the PAN band (8^{th} band) with the MS(Multi-Spectral) bands. This technique is also referred to as the pansharpening method (Aiazzi et al., 2009). Pansharpening carried out as Landsat series images have a limited spatial resolution (30 m) of MS image (Liu et al., 2017) (Pardo-Pascual et al., 2012). After the pan-sharpening, the data become a high resolution.

From the latest data, the shoreline was digitised for the entire district. After the on-screen digitisation, a 5km buffer line from the digitised shoreline was created to make the boundary. After making the boundary, the data were masked and extracted. The extracted data sets were classified using the classifier tool in ArcGIS 10.3. Spectral signatures were carefully selected for the LULC classification. Totally 12 number of classes has been worked out for the study (Table 3)

Sl. No.	Name of LULC
1	Crop Cultivable Land
2	Barren Land
3	Beach face Land Cover
4	Dune Vegetation
5	Fallow Land
6	Plantation
7	River
8	Saline Water Body
9	Salt Pan
10	Settlement & Built ups

11	Water Body
12	Beach Mining

Table 3: Name of the LULC classes

The above classes were performed according to the created spectral signatures. Supervised classification was carried out; in this study, the Maximum Likelihood Classifier (MLC) (Settle & Briggs, 1987) was adopted. The classification is based on the defined spectral signatures for the supervised classification representative samples needed for each land cover and the land-use class. In this study, twelve different units were classified, reported by Kaliraj et al. (2017), who did a similar study in this region. The classified classes: Crop Cultivable Land, Barren Land, Beachface Land Cover, Dune Vegetation, Fallow Land, Plantation, River, Saline Water Body, Salt Pan, Settlement & Built-ups, Water Body, Beach Mining.
With the complexity of digital classification, there is more of a need to assess the reliability of the results (Congalton, 1991).so after the classification, the accuracy assessment has been performed with the help of field observed GPS points. For each class, 10 points were marked from the field using a handheld GPS. Producer accuracy, user accuracy, overall accuracy were obtained from the accuracy assessment. The error matrix technique was carried out for the reliability of the result and for validating the remote sensing classification. Error matrix (confusion matrix) – compares ground truth data with results of classification.

3. RESULT AND DISCUSSION

Landuse and Landcover classification were done for the selected three years (2013,2017, 2021) for the coastal Kanyakumari district using the Landsat 8 data.

Sl. No.	Land use and Landcover feature	2013	
		Area (km^2)	% of distribution
1	Water bodies	3.078168032	1.01
2	Salt pan	1.164451755	0.38
3	Saline water bodies	2.673522314	0.87
4	River	1.975460185	0.65
5	Plantation	105.7833508	34.73
6	Fallow land	9.791039139	3.21
7	Dune vegetation	8.75392697	2.87
8	Crop cultivable land	58.80147754	19.30
9	Built ups	61.09068414	20.06
10	Beachface land cover	13.7309742	4.51
11	Beach mining	3.859117094	1.26
12	Barren land	33.86435013	11.12

Table 4 LULC feature's area and percentage of distribution in 2013

Sl. No.	Land use and Landcover feature	2017	
		Area (km^2)	% of distribution
1	Water bodies	1.35348452	0.44
2	Salt pan	3.932069661	1.29

3	Saline water bodies	3.622859918	1.19
4	River	1.883442182	0.62
5	Plantation	109.2680322	35.87
6	Fallow land	9.231803592	3.03
7	Dune vegetation	9.179554583	3.01
8	Crop cultivable land	62.26056047	20.44
9	Built ups	79.25017872	26.02
10	Beachface land cover	2.139768275	0.70
11	Beach mining	5.452687798	1.79
12	Barren land	16.99553131	5.58

Table 5 LULC feature's area and percentage of distribution in 2017

Sl. No.	Land use and Landcover feature	2021	
		Area (km^2)	% of distribution
1	Water bodies	1.91931429	0.63
2	Salt pan	8.176454188	2.68
3	Saline water bodies	0.151578443	0.05
4	River	2.193640532	0.72
5	Plantation	114.0802638	37.46
6	Fallow land	15.83248791	5.20
7	Dune vegetation	6.240357173	2.05
8	Crop cultivable land	40.45652337	13.28
9	Built ups	89.76390683	29.47
10	Beachface land cover	6.609733459	2.17
11	Beach mining	4.988608544	1.64
12	Barren land	14.15985289	4.65

Table 6 LULU feature's area and percentage of distribution in 2021

Change in the area (km^2)	Change in % of the distribution
-1.724683512	-0.57
2.767617906	0.91
0.949337604	0.32
-0.092018003	-0.03
3.4846814	1.14
-0.559235547	-0.18
0.425627613	0.14
3.45908293	1.14
18.15949458	5.96
-11.5912054202	-3.81
1.593570704	0.53
-16.86881882	-5.54

Table 7 Change in area of the LULC for the years between 2013-2017

Change in the area (km^2)	Change in % of the distribution
0.56582977	0.19

4.244384527	1.39
-3.471281475	-1.14
0.31019835	0.1
4.8122316	1.59
6.600684318	2.17
-2.93919741	-0.96
-21.8040371	-7.16
10.51372811	3.45
4.469965184	1.47
-0.464079254	-0.15
-2.83567842	-0.93

Table 8 Change in area of the LULC for the years between 2017-2021

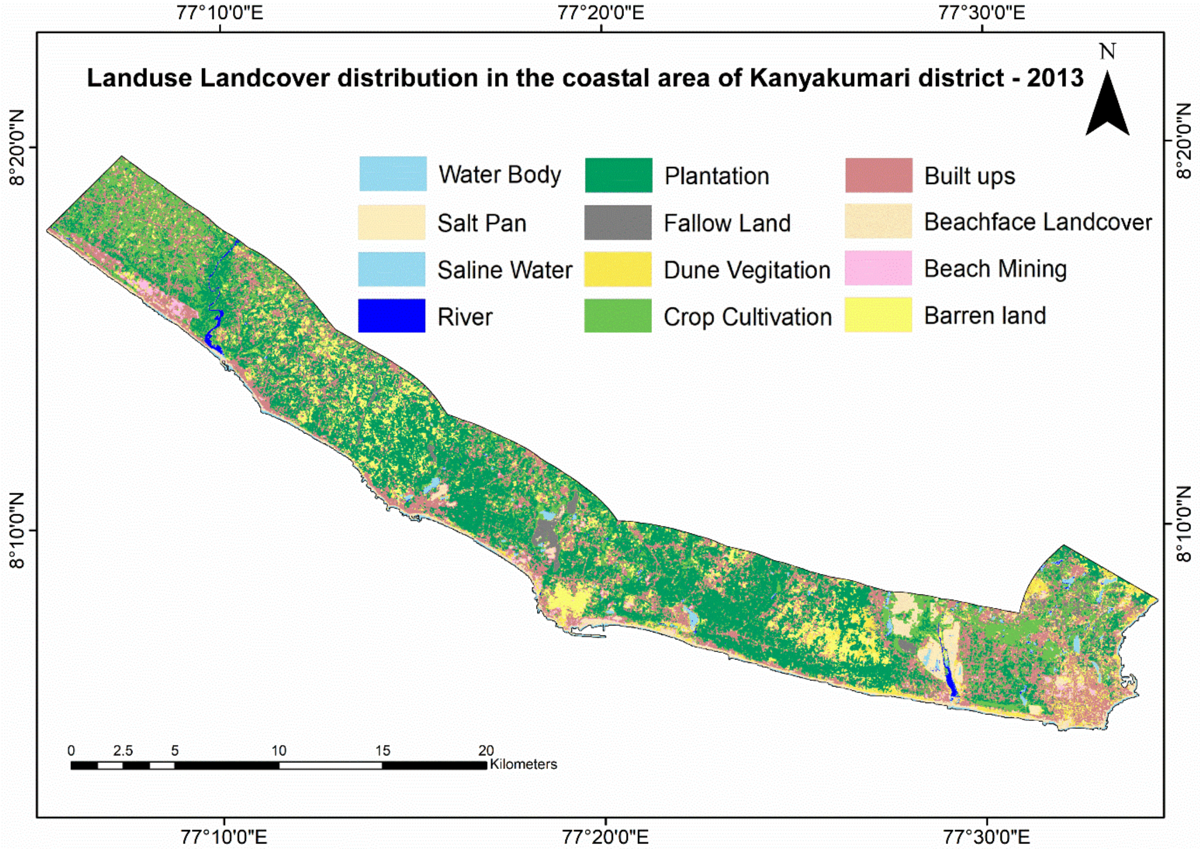

Figure 4 LULC changes of the year 2013

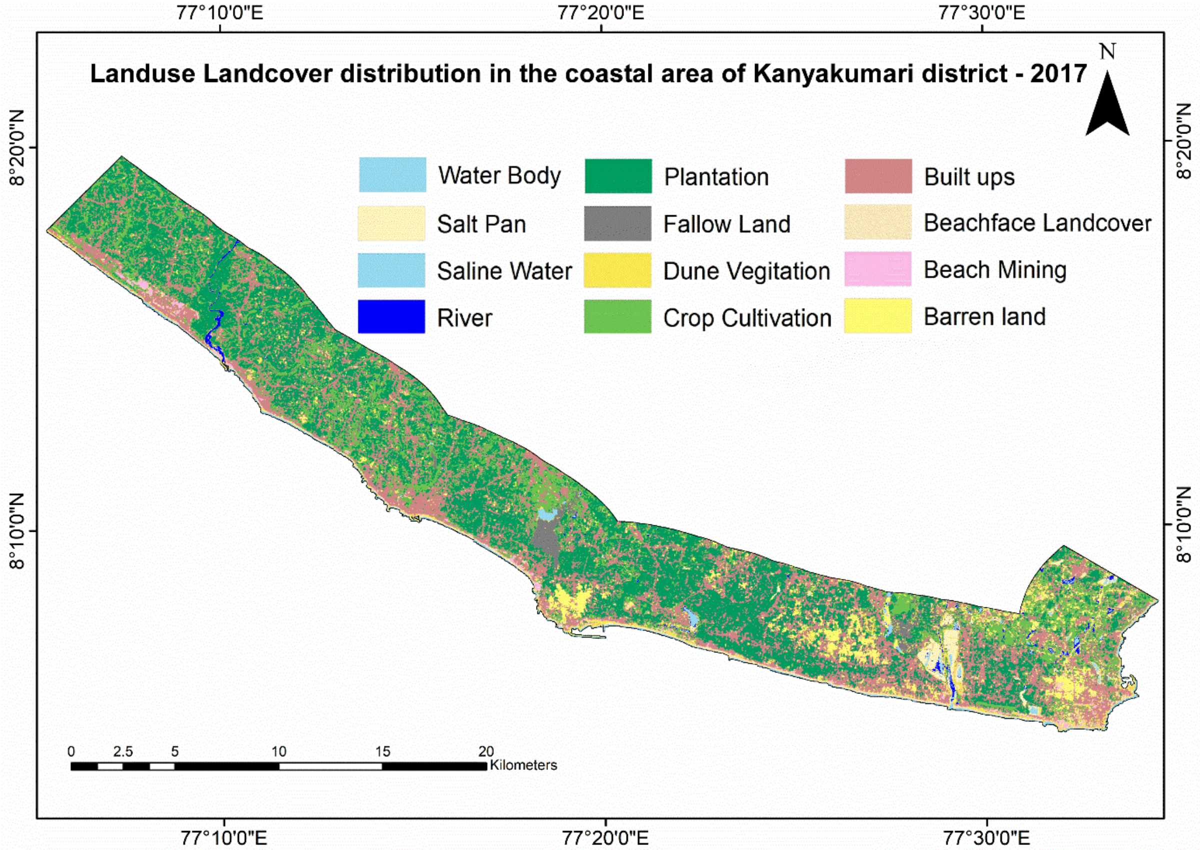

Figure 5 LULC changes of the year 2017

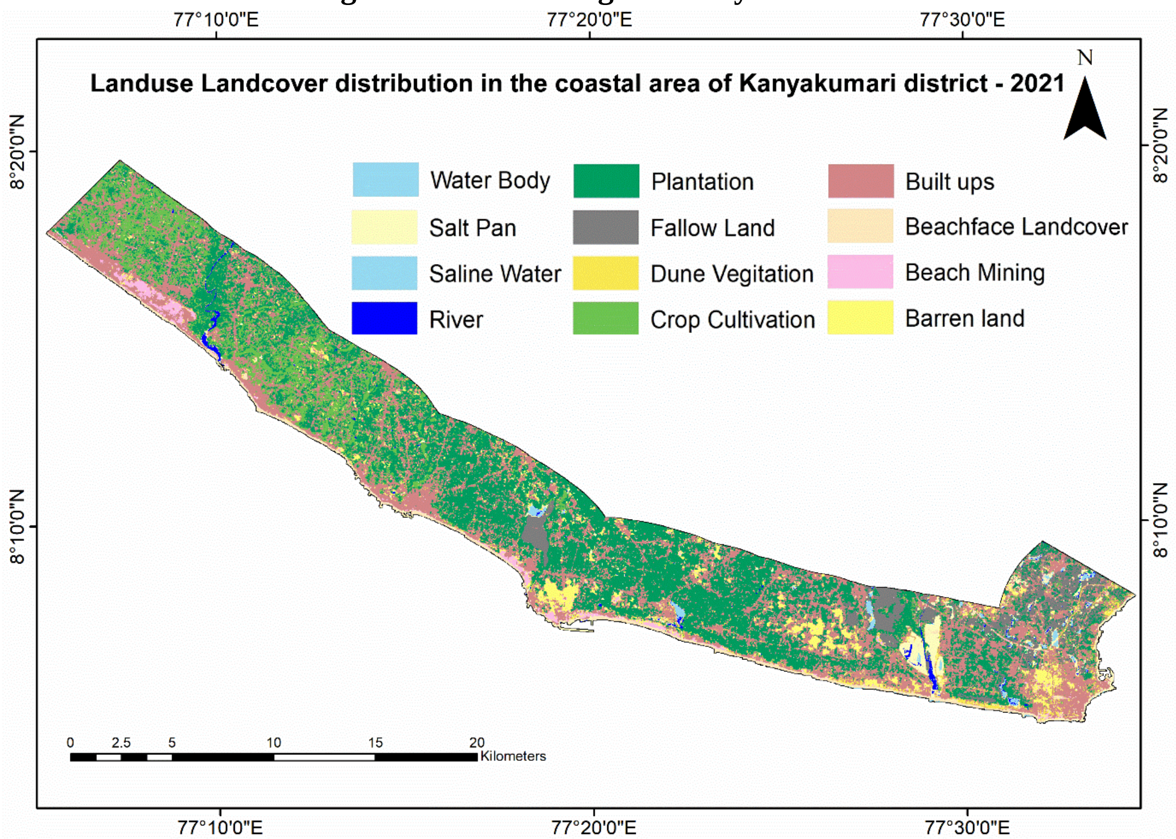

Figure 6 LULC changes of the year 2021

Figure 7 Field Photographs

4.1.1 Crop Cultivable Land

The cultivatable lands are spread mainly alongside the riverbanks and lakesides of the study area. In the western side of the Thengapattanam, more cultivable lands are present as the River Tamiraparani (Figure 4,5,6) flows through the particular part of the study area. In the study area, cultivatable cropland widened from 2013 to 2017 (Table 7). In the year 2013, the cultivatable cropland was around 58.8 km^2(Table 4). Notably, the cultivatable cropland was increased in 2017, and the total area in 2017 was 62.26 km^2(Table 5). But at the same time, the size of cultivatable cropland in the district's coastal area drastically changed in 2021, and it decreased in the total area about 20 km^2 from the year 2017(Table 8). The total area of the cultivatable cropland in 2021 was calculated as 40.45 km^2(Table 6). The main reason for the change in the cropland is urbanisation, which unavoidably occupies the world's most valuable croplands (Qiu et al., 2020; Seto & Ramankutty, 2016; Song et al., 2018; van Vliet, 2019).

4.1.2 Barren Land

Barren land is a non-cultivable land with or without scrubs. Teri dunes from the study area were mainly barren land (S Kaliraj *et al.*, 2017). Muttom, Manakudi, to Kovalam areas have the Teri dunes, categorised as bare land. Most barren lands are found on the periphery of urban areas(Lu *et al.*, 2011). Year by year, barren land in the study area was decreasing in its area. In 2013, the barren land occupied 33.86km^2 (Table 4) in the study area. In 2017, the classified image (Figure 5) shows that the barren land dramatically decreased in its area by 16.86 km^2(Table 5). As per the 2021 classified image, the study area's barren lands total area was identified as 14.16 km^2(Table 6). The main reason behind reducing the bare land is found as the built-up areas in the study area.

4.1.3 Beachface Land Cover

Beachface land cover includes sandy beaches, dunes and associated landforms within the nearshore area. The features of this class are undergone a high rate of changes over time due to the marine and coastal Processes and other anthropogenic activities (S. Kaliraj *et al.*, 2017). As per 2013, the feature's area was 13.73km^2(Table 4); meanwhile, in 2017, the feature's total area was around 2.14km^2(Table 5). So, between 2013 to 2017, the beachface landcover lose 11.59km^2 in its area (Table 7). In 2021, the feature had increased its area by 4.47km^2(Table 8), and the total area was 6.61km^2. Erayumanthurai, Pillaithoppu, Colachel, Ganapathipuram, Rajakamangalam, these areas have the beachface landcover on their coast.

4.1.4 Dune Cover Vegetation

Shrubs, grasses, bushes, casuarinas are the primary dune vegetative cover in the coastal area (Figure 7b). From 2013 to 2017, the dune vegetative cover was increased in various parts of the study area. The area changed from 8.75km^2 to 9.18km^2, with a total gain in the area of 0.43 km^2(Table 5). The casuarina tree afforestation could be the reason behind the increase of the dune cover vegetation from 2013 to 2017. From Mandaikadu to Manavazhakurichi, the afforestation took place after the placer mining in those areas. But from 2017 to 2021, dune vegetation has lost its size by 2.94km^2 with a current area of 6. 24km2.In the study area, the Dune cover vegetative can find between the Manakudi to Kovalam villages. In Sothavillai, Sanguthurai, Pallam areas have a long patch of dune formations with shrubs.

4.1.5 Fallow Land

Fallow land is all cultivatable land included in the crop rotation system or maintained in good agricultural and environmental conditions. Fallowing the land allows it to regain and store organic material while retaining moisture and disrupting pathogens' lifecycles by eliminating their hosts. In the Study area by 2013, the total area covered by fallow land is 9.79 km^2(Table 4). It slowly kept decreasing in its size, and by 2017, it covers an area of 9.23 km^{2,} i.e., it fell by 0.56 km^2. But, from 2017 to 2021, it increased significantly by 6.60 km^2(Table 8). In 2021, the total area of fallow land is 15.83 km^2(Table 6): Pazhayar rivers estuary area, the larger fallow lands found in Kanyakumari (S Kaliraj *et al.*, 2017).

4.1.6 Plantation

Coconut palm reduces the effect of erosive forces using their root system and foliage (Pal, 2018). In the year 2013, the area covered by plantations is about 105.78 km^2(Table 4). This plantation area frequently increased by 3.48 km^2, and in 2017 the total area covered by it is 109.26 km^2(Table 5). Between 2017-2021, the plantation area kept on increasing to 114.08 km^2(Table 6). Comparing with 2017, In 2021, the plantation area has increased by 4. 81 km^2(Table 8).

4.1.7 Rivers and Water Bodies

Three major rivers flow in the study area. Thamirabarani, Pazhaiyar, Valliyar (Figure 7d) are those rivers. These are the primary source for the agriculture activities in the study area. So, the plantation and the croplands are primarily found in the banks of these rivers. In 2013, the area covered by the river in the study area was 1.96 km^2(Table 4). This area remained more constant with some minor downfall of 0.095 km^2, i.e., by 2017, the total area covered by the river is 1.88 km^2. Then again, the area kept on increasing. From 2017 to 2021, the areal extend raised by 0.31 km^2. As of 2021, the total areal growth of the river is calculated as 2.19 km^2(Table 6).

And also, lakes and ponds are found all over the study area. North of the Kanyakumari area can find a significant number of lakes that are irrigating those nearby areas. In 2013 the waterbodies occupied a total of 3km^2 of the study area. In 2017 it decreased 1.72 km^2 from the year 2013 because of the human encroachment activities. In 2021, the water bodies' total area increases because the local government takes measurements to dredge and maintain the water bodies. In 2021 the waterbodies total area was found as 1.9 km^2(Table 6)

4.1.8 Saline Water and Salt pans

Saltpans (Figure 7c) and saltwater bodies are located mainly throughout the estuaries and backwaters in the study area. From 2013 to 2017, the saltpans have expanded in spatial extent from 1.16 km^2 to 3.93 km^2(Table 7). Again, from 2017 to 2021, the saltpan area is extended mainly in the study area (Table 8). The total area of the saltpan found in 2021 is about 8.17km^2(Table 6). The saltpans are mainly located in the Pazhayar estuary near Manakudi (Figure 7c).

The saltwater bodies beside the backwaters are influenced by the human activities forming the saltpans in most areas. So, the saltwater body shows a decreasing trend in 2021 compared to 2017. It decreased vastly in its size from 3.62km^2 to 0.015km^2(Table 8). Simultaneously, a few freshwater ponds in the backshore parts of Kovalam, Rajakkamangalamthurai, Manavalakurichi, and Thengapattinam coastal areas are altered into saltwater bodies seawater intrusion (Hentry *et al.*, 2010). The increase of area in saltwater bodies in some areas causes groundwater pollution through the free movement of seawater to the freshwater aquifers. But in most places, the amount of saltwater body is diminished because of the excellent rainfall and measured activities of local governments.

4.1.9 Settlement & Built ups

Settlements are primarily defined as a city, town, village, or other groupings of structures where people live and work (Claramunt, Levashkin and Bertolotto, 2011). Roads, enclosures, field systems, boundary banks and ditches, ponds, parks and woods, wind and watermills, manor buildings, moats, and churches are standard features of a settlement (Gardiner, 2006). According to the 2011 census, the population density of the Kanyakumari district's coastal ar ea is 1005 people per square kilometre (Chandramouli and General, 2011), which is very dense compared to other districts is raised between 2013 and 2021. The settlement areas are closely tied to the increase of the people in these areas, which grows primarily due to improved access to daily necessities. The spatial extent of settlements and built-ups is 61.09 km^2 in 2013, and it covers 20.06% of the total study area (Table 4). Due to outspreading settlements in rural and urban areas, this is increased to 79.25 km^2, equivalent to 26.02% of the total area in 2017 (Table 5). By 2021, the Built-up area is increased to 89.76 km2 which is 29.47 % of the study area. Most of the beachface landforms, cultivable land, fallow land and barren land are encroached by the settlements from 2013 to 2021. In the eastern part of the study area, the dune complexes and coastal plains are transformed into built-ups, factories and resorts; and the western parts near Midalam, Colachel coastal areas, the fertile agricultural land, fallow land and few areas of barren lands are utilised for the expansion of settlement areas. In Muttom, many Teri sand dune areas were transformed into the collages and the other settlement areas. It is noticed that the encroachment of coastal land cover for settlements and built-ups on a large scale negatively impacts the coastal ecology and increases the rate of vulnerability to the coastal region.

4.1.10 Beach Mining

The beach mining areas are primarily in the Manavalakurichi-Mandaikadu coastal area in the study area (Figure 7a). The spatial extent of beach mines is 3.85 km^{2} in 2013, 5.45 km^{2} in 2017 and 4.98 km^{2} in 2021(Table 4,5 and 6). A few ditched placer mining pits are predominantly found along with the working mines in Manavalakurichi-Mandaikadu coastal areas. Removal of sand due to placer mining is a pathway for intruding seawater to the inland aquifers (Kaliraj, Chandrasekar and Magesh, 2014). Besides, some parts of granite quarries are noticed near Inayamputhenthurai and Thengapattinam coastal areas.

4. RESULT

The total area of the cultivatable cropland in 2021 was 40.45 km^{2} which is 18.35 km^{2,} less than 2013. In 2013, the barren land occupied 33.86km^{2,} but in the 2021 classified image, the study area's barren lands total area was 14.16 km^{2}. The beachface landcover area in 2013 was 13.73km^{2} that changed to 6.61km^{2} in 2021. As per the year 2013, the dune cover vegetation's area was 8.75 km$^{2;}$ it is also reduced in its area by the time of 2021, the dune cover vegetation was occupied 6.24km^{2}. The cultivable cropland, barren land, beachface landcover, and dune cover vegetation decrease because of urbanisation's rapid growth. By 2013, the total area covered by fallow land is 9.79 km^{2}. It slowly kept on decreasing in its area, and by 2017, it covers an area of 9.23 km^{2,} i.e., it fell by 0.56 km^{2}. But, from 2017 to 2021, it increased significantly by 6.60 km^{2}. In 2021, the total area of fallow land is 15.83 km^{2}. In the year 2013, the area covered by plantations is about 105.78 km^{2}. The plantation area kept on increasing to 114.08 km^{2} in 2021. The spatial area of the saltpans in the study area by 2013 is 1.16 km^{2} which increased rapidly to 8.17km^{2} in 2021. The spatial extent of settlements and built-ups is 61.09 km^{2} in 2013, and it covers 20.06% of the total study area. By 2021, the Built-up area is increased to 89.76 km2 which is 29.47 % of the study area. Most of the beachface landforms, cultivable land, fallow land and barren land are encroached by the settlements from 2013 to 2021. The spatial extent of beach mines is 3.85 km^{2} in 2013, 5.45 km^{2} in 2017 and 4.98 km^{2} in 2021.

The Fallow land, the plantation, the saltpans, the built-up area and the beach mining areas show an increasing trend in the study area. The plantation, the fallow land and the beach mining only increase a little in their area, but the saltpans and the built-up areas increase rapidly. The rapid increase of the saltpans and the built-up area shows rapid urbanization in the study area.

4.3 Accuracy assessment

The classified image producer’s accuracy, user accuracy, and overall accuracy have been found to validate the classified imagery. Every feature 10 GPS points have been taken using these points; this accuracy assessment was carried out in the 2021 classified imagery. The true value and classified value are given in Table 9.

Class Name	TRUTH1 River	TRUTH2 Built ups	TRUTH3 Saline water	TRUTH4 Beach mining	TRUTH5 Water body	TRUTH6 Fallow land	TRUTH7 Crop cultivable land	TRUTH8 Salt pan	TRUTH9 Plantation	TRUTH10 Beachface land cover	TRUTH11 Barren land	TRUTH12 Dune vegetation	Row Total
River	**10**	0	0	0	0	0	0	0	0	0	0	0	**10**
Built ups	0	**10**	0	1	0	0	0	0	1	0	1	0	**13**
Saline water	0	0	**9**	0	0	0	0	0	0	0	0	0	**9**
Beach mining	0	0	0	**9**	0	0	0	0	0	1	0	0	**10**
Water body	0	0	0	0	**10**	0	0	0	0	0	0	0	**10**
Fallow land	0	0	0	0	0	**10**	0	0	1	0	0	0	**11**
Crop cultivable land	0	0	0	0	0	0	**10**	0	0	0	0	0	**10**
Salt pan	0	0	0	0	0	0	0	**10**	0	0	0	0	**10**
Plantation	0	0	0	0	0	0	0	0	**8**	0	0	0	**8**
Beachface land cover	0	0	1	0	0	0	0	0	0	**8**	0	0	**9**

Barren land	0	0	0	0	0	0	0	0	0	1	**9**	0	**10**
Dune vegetation	0	0	0	0	0	0	0	0	0	0	0	**10**	**10**
Column Total	**10**	**10**	**10**	**10**	**10**	**10**	**10**	**10**	**10**	**10**	**10**	**10**	**120**

Table 1 Accuracy assessment

1 Producer Accuracy

Producers Accuracy measure indicates the probability of a correctly classified reference pixel and measures omission error (Congalton, 1991). The producer's accuracy is identified using the following formula for each class.

Truth / Column Total

Producers Accuracy
River = 10/10 which is 1.00
Built ups = 10/10 which is 1.00
Saline water = 9/10 which is 0.90
Beach mining = 9/10 which is 0.90
Water body = 10/10 which is 1.00
Fallow land = 10/10 which is 1.00
Crop cultivable land = 10/10 which is 1.00
Salt pan = 10/10 which is 1.00
Plantation = 8/10 which is 0.80
Beachface land cover = 8/10 which is 0.80
Barren land = 9/10 which is 0.90
Dune vegetation = 10/10 which is 1.00

2 Users Accuracy

The Users Accuracy reveals the possibility that a pixel classified on the image represents that category on the ground (Story and Congalton, 1986). The user's accuracy is calculated using the following formula for each class.

Truth/row total

Users' accuracy
River = 10/10, which is 1.00
Built ups = 10/13 which is 0.77
Saline water = 9/9, which is 1.00
Beach mining = 9/10, which is 0.90
Waterbody = 10/10, which is 1.00
Fallow land = 10/11, which is 0.91
Crop cultivable land = 10/10 which is 1.00
Salt pan = 10/10, which is 1.00
Plantation = 8/8 which is 1.00

Beachface land cover = 8/9, which is 0.89
Barren land = 9/10 which is 0.90
Dune vegetation = 10/10 which is 1.00

3 Overall Accuracy

The overall accuracy is calculated using the following formula.

Sum of the total Truth/row total

Sum of the total truth = 113
Row total = 120
Hence the overall accuracy of the supervised classification result of the study area is found as **0.94.**

5. CONCLUSION:

The LULC changes study is crucial to understand the hazards and vulnerability of the study area because of the natural and anthropogenic activities. Optical remote sensing and the Geographic Information System provide an effective platform for evaluating LULC changes and their alterations over the period.

In this study, the authors found out that the cultivable cropland, barren land, beachface landcover, dune cover vegetation decrease because of the rapid growth of urbanization from 2013 to 2021. At the same time, The Fallow land, the plantation, the saltpans, the built-up area and the beach mining areas show an increasing trend in the study area from 2013 to 2021. The plantation, the fallow land and the beach mining only increase a little in their area, but the saltpans and the built-up areas increase rapidly. The rapid increase of the saltpans and the built-up area shows rapid urbanization in the study area. The saltpans are raised in the area due to Anthropogenic activities.

It is observed that the many LULC features were severely damaged during the year 2017 due to the effect of very severe Cyclonic Storm Ockhi that occurred in November 2017. The unfettered changes in the LULC feature are alarming the coastal vulnerability in the Kanyakumari districts coastal villages. This study offers pilot information for sustainable coastal management and planning to decrease coastal regions' risk and vulnerability.

6. REFERENCES:

[1] Aiazzi, B., Baronti, S., Lotti, F., & Selva, M. (2009). A comparison between global and context-adaptive pansharpening of multispectral images. *IEEE Geoscience and Remote Sensing Letters*, *6*(2), 302–306.

[2] Alam, S. M. N., Demaine, H., & Phillips, M. J. (2002). Land use diversity in south western coastal areas of Bangladesh. *The Land*, *6*(3), 173–184.

[3] Attri, P., Chaudhry, S., & Sharma, S. (2015). Remote Sensing & GIS based Approaches for LULC Change Detection - A Review. *International Journal of Current Engineering and Technology*.

[4] Avery, T. E., & Berlin, G. L. (1992). Fundamentals of remote sensing and airphoto interpretation. Macmillan.

[5] Chandramouli, C., & General, R. (2011). Census of india 2011. *Provisional Population Totals. New Delhi: Government of India*, 409–413.

[6] Chandrasekar, N. (2013). Coastal Vulnerability and Shoreline Changes for Southern Tip of India-Remote Sensing and GIS Approach. *Journal of Earth Science & Climatic Change*. https://doi.org/10.4172/2157-7617.1000144

[7] Chandrasekar, N., Cherian, A., Rajamanickam, M., & Rajamanickam, G. V. (2000). Coastal landform mapping between Tuticorin and Vaippar using IRS-IC data. *Indian Journal of Geomorphology*, *5*(1&2), 114–120.

[8] Chandrasekharan, S. (2001). Heavy minerals in the beach and coastal red sands (Teris) of Tamil Nadu. *Explor. Research Atomic Minerals*, *13*, 87–109.

[9] Claramunt, C., Levashkin, S., & Bertolotto, M. (2011). GeoSpatial Semantics: 4th International Conference, GeoS 2011, Brest, France, May 12-13, 2011, Proceedings. Springer Science & Business Media.

[10] Congalton, R. G. (1991). A review of assessing the accuracy of classifications of remotely sensed data. *Remote Sensing of Environment*. https://doi.org/10.1016/0034-4257(91)90048-B

[11] Deng, Z., Zhu, X., He, Q., & Tang, L. (2019). Land use/land cover classification using time series Landsat 8 images in a heavily urbanised area. *Advances in Space Research*, *63*(7), 2144–2154.

[12] Gardiner, M. (2006). Review of medieval settlement research, 1996–2006. *Medieval Settlement Research Group Annual Report*, *21*, 22–28.

[13] Gilmore, M. S., Wilson, E. H., Barrett, N., Civco, D. L., Prisloe, S., Hurd, J. D., & Chadwick, C. (2008). Integrating multi-temporal spectral and structural information to map wetland vegetation in a lower Connecticut River tidal marsh. *Remote Sensing of Environment*, *112*(11), 4048–4060.

[14] Hentry, C., Chandrasekar, N., Saravanan, S., & Sahayam, J. D. (2010). Influence of geomorphology and bathymetry on the effects of the 2004 tsunami at Colachel, South India. *Bulletin of Engineering Geology and the Environment*, *69*(3), 431–442.

[15] Hua, L., Zhang, X., Chen, X., Yin, K., & Tang, L. (2017). A feature-based approach of decision tree classification to map time series urban land use and land cover with Landsat 5 TM and Landsat 8 OLI in a Coastal City, China. *ISPRS International Journal of Geo-Information*, *6*(11), 331.

[16] Jaiswal, R. K., Saxena, R., & Mukherjee, S. (1999). Application of remote sensing technology for land use/land cover change analysis. *Journal of the Indian Society of Remote Sensing*, *27*(2), 123–128. https://doi.org/10.1007/BF02990808

[17] Jayappa, K. S., Mitra, D., & Mishra, A. K. (2006). Coastal geomorphological and land-use and land-cover study of Sagar Island, Bay of Bengal (India) using remotely sensed data. *International Journal of Remote Sensing*, *27*(17), 3671–3682.

[18] Kaliraj, S., Chandrasekar, N., & Magesh, N. S. (2014). Impacts of wave energy and littoral currents on shoreline erosion/accretion along the southwest coast of Kanyakumari, Tamil Nadu using DSAS and geospatial technology. *Environmental Earth Sciences*, *71*(10), 4523–4542.

[19] Kaliraj, S., Chandrasekar, N., & Magesh, N. S. (2015). Evaluation of coastal erosion and accretion processes along the southwest coast of Kanyakumari, Tamil Nadu using geospatial techniques. *Arabian Journal of Geosciences*, *8*(1), 239–253.

[20] Kaliraj, S., Chandrasekar, N., Ramachandran, K. K., Srinivas, Y., & Saravanan, S. (2017a). Coastal landuse and land cover change and transformations of Kanyakumari coast, India using remote sensing and GIS. *The Egyptian Journal of Remote Sensing and Space Science*, *20*(2), 169–185.

[21] Kaliraj, S., Chandrasekar, N., Ramachandran, K. K., Srinivas, Y., & Saravanan, S. (2017b). Coastal landuse and land cover change and transformations of Kanyakumari coast, India using remote sensing and GIS. *Egyptian Journal of Remote Sensing and Space Science*. https://doi.org/10.1016/j.ejrs.2017.04.003

[22] Kurt, S. (2013). Land use changes in Istanbul's Black Sea coastal regions between 1987 and 2007. *Journal of Geographical Sciences*. https://doi.org/10.1007/s11442-013-1009-7
[23] Liu, Y., Wang, X., Ling, F., Xu, S., & Wang, C. (2017). Analysis of coastline extraction from Landsat-8 OLI imagery. *Water*, *9*(11), 816.
[24] Lu, Q., Liang, F., Bi, X., Duffy, R., & Zhao, Z. (2011). Effects of urbanisation and industrialisation on agricultural land use in Shandong Peninsula of China. *Ecological Indicators*, *11*(6), 1710–1714.
[25] Mujabar, P. S., & Chandrasekar, N. (2012). Dynamics of coastal landform features along the southern Tamil Nadu of India by using remote sensing and Geographic Information System. *Geocarto International*, *27*(4), 347–370.
[26] Natesan, U., & Parthasarathy, A. (2010). The potential impacts of sea level rise along the coastal zone of Kanyakumari District in Tamilnadu, India. *Journal of Coastal Conservation*, *14*(3), 207–214. https://doi.org/10.1007/s11852-010-0103-6
[27] Nguyen, H. T. T., Doan, T. M., & Radeloff, V. (2018). Applying random forest classification to map land use/land cover using landsat 8 OLI. *Int. Arch. Photogramm. Remote Sens. Spat. Inf. Sci*, 363–367.
[28] Pal, R. K. (2018). Role of coconut in reducing soil erosion in East & North East India. *Indian Coconut Journal*, *61*(2), 4–5.
[29] Pardo-Pascual, J. E., Almonacid-Caballer, J., Ruiz, L. A., & Palomar-Vázquez, J. (2012). Automatic extraction of shorelines from Landsat TM and ETM+ multi-temporal images with subpixel precision. *Remote Sensing of Environment*, *123*, 1–11.
[30] Qiu, B., Li, H., Tang, Z., Chen, C., & Berry, J. (2020). How cropland losses shaped by unbalanced urbanisation process? *Land Use Policy*, *96*, 104715.
[31] Roy, P. S., & Roy, A. (2010). Land use and land cover change in India: A remote sensing & GIS prespective. In *Journal of the Indian Institute of Science*.
[32] Santhiya, G. (2010). Mapping of Landuse/Landcover Changes of Chennai Coast and Issues related to Coastal Environment Using Remote Sensing and GIS. *International Journal of Geomatics and Geosciences*, *1*(3), 563–576. http://www.indianjournals.com/ijor.aspx?target=ijor:ijggs&volume=1&issue=3&article=023
[33] Sekertekin, A., Marangoz, A. M., & Akcin, H. (2017). Pixel-based classification analysis of land use land cover using Sentinel-2 and Landsat-8 data. *Int. Arch. Photogramm. Remote Sens. Spat. Inf. Sci*, *42*, 91–93.
[34] Seto, K. C., & Ramankutty, N. (2016). Hidden linkages between urbanisation and food systems. *Science*, *352*(6288), 943–945.
[35] Settle, J. J., & Briggs, S. A. (1987). Fast maximum likelihood classification of remotely-sensed imagery. *International Journal of Remote Sensing*. https://doi.org/10.1080/01431168708948683
[36] Sharma, J., Prasad, R., Mishra, V. N., Yadav, V. P., & Bala, R. (2018). Land Use and Land Cover Classification of Multispectral LANDSAT-8 Satellite Imagery Using Discrete Wavelet Transform. *International Archives of the Photogrammetry, Remote Sensing and Spatial Information Sciences, 42*(5).
[37] Song, X.-P., Hansen, M. C., Stehman, S. V, Potapov, P. V, Tyukavina, A., Vermote, E. F., & Townshend, J. R. (2018). Global land change from 1982 to 2016. *Nature*, *560*(7720), 639–643.
[38] Stanley Raj, A., Hudson Oliver, D., Srinivas, Y., & Viswanath, J. (2017). Wavelet based analysis on rainfall and water table depth forecasting using Neural Networks in Kanyakumari district, Tamil Nadu, India. *Groundwater for Sustainable Development*. https://doi.org/10.1016/j.gsd.2017.06.009

[39] van Vliet, J. (2019). Direct and indirect loss of natural area from urban expansion. *Nature Sustainability*, *2*(8), 755–763.
[40] Wickware, G. M., & Howarth, P. J. (1981). Change detection in the Peace—Athabasca delta using digital Landsat data. *Remote Sensing of Environment*, *11*, 9–25.
[41] Xiuwan, C. (2002). Using remote sensing and GIS to analyse land cover change and its impacts on regional sustainable development. *International Journal of Remote Sensing*. https://doi.org/10.1080/01431160010007051
[42] Xu, X., Peng, H., Xu, Q., Xiao, H., & Benoit, G. (2009). Land changes and conflicts coordination in coastal urbanisation: A case study of the shandong peninsula in china. *Coastal Management*. https://doi.org/10.1080/08920750802612788